

## Phonon superlattice transport

Per Hyldgaard\* and G. D. Mahan

*Department of Physics and Astronomy, University of Tennessee, Knoxville, Tennessee 37996-1200  
and Solid State Division, P.O. Box 2008, Oak Ridge National Laboratory, Oak Ridge, Tennessee 37831-6030*

(Received 9 July 1997)

We predict in Si/Ge superlattices a dramatic high-temperature suppression of the perpendicular thermal transport. Total internal reflection confines the superlattice modes and significantly reduces the average group velocity at nonzero in-plane momenta. These consequences of the acoustic mismatch cause at high temperatures an order-of-magnitude reduction in the ratio of superlattice thermal conductivity to phonon relaxation time. [S0163-1829(97)07441-9]

The observed<sup>1,2</sup> reduction of the in-plane thermal conductivity in long-period GaAs/AlAs superlattices implies a potentially attractive application for semiconductor heterostructures in thermoelectric devices.<sup>3</sup> The in-plane superlattice thermal transport has consequently been the focus of theoretical investigations.<sup>4,5</sup>

Two recent experiments<sup>6,7</sup> also report a dramatic reduction for the thermal transport perpendicular to the GaAs/AlAs superlattice interfaces. The perpendicular thermal conductivity  $\kappa_{\text{SL}}$  reported in Ref. 7 exhibits an order-of-magnitude room-temperature reduction compared with that of bulk GaAs and cannot be explained as alloy scattering.

A very recent paper<sup>8</sup> investigates this microscopic heat transfer and reports a Boltzmann transport calculation based on a *bulk* phonon dispersion in each of the superlattice layers. Assuming complete diffusive scattering<sup>9,4,5</sup> at every interface, that is, a very strong reduction in the effective phonon relaxation time  $\tau_{\text{SL}}$ , it is possible to account for the observed<sup>6,7</sup> reduction in the perpendicular superlattice thermal conductivity.<sup>8</sup>

We believe it essential, however, to describe the superlattice thermal transport  $\kappa_{\text{SL}}$  across the increasingly perfect interfaces based instead on the *superlattice-phonon* spectrum. Total internal reflection results with a finite acoustic mismatch difference in material sound velocities in a significant suppression of the phonon flux across an individual heterostructure interface.<sup>10</sup> We must therefore expect a corresponding reduction in the perpendicular group velocity of the superlattice phonon modes, that is, an effective modal confinement. Below we document how the acoustic mismatch causes such a modal confinement and produces a superlattice phonon spectrum qualitatively different from those of the individual bulk layers.

Early one-dimensional model investigations yielded phonon spectra for GaAs/AlAs (Refs. 11 and 12) and Si/Ge (Ref. 13) superlattice modes propagating at right angles to the interfaces, i.e., with zero in-plane momentum,  $\mathbf{q} \equiv 0$ . Such modes can be probed optically and as a function of perpendicular momentum  $k$  using ultrasound.<sup>11</sup> The increased umklapp scattering of the zone-folded  $\mathbf{q} = 0$  GaAs/AlAs superlattice modes causes a small (<25%) reduction in the effective phonon relaxation time  $\tau_{\text{SL}}$  and thus in the thermal conductivity.<sup>14</sup>

More recently there have been several three-dimensional calculations of the superlattice phonons identifying both the

effects of strain<sup>15</sup> and a finite interface disorder.<sup>16</sup> Most investigations report the dispersion,  $\omega(\mathbf{q}, k)$ , of superlattice modes propagating either entirely within the superlattice planes,  $k \equiv 0$ , or at right angles to the interfaces,  $\mathbf{q} \equiv 0$ . None of these studies, however, directly illustrate the effective modal confinement,  $\partial\omega(k; \mathbf{q})/\partial k \approx 0$ , arising at  $\mathbf{q} \neq 0$ .

In this paper we attempt such an illustration and also explore the important consequences for the perpendicular thermal conductivity  $\kappa_{\text{SL}}$  of Si/Ge superlattices. We assume perfect interfaces and use a simple-cubic effective phonon model<sup>17</sup> to (i) document how the finite acoustic mismatch ensures a dramatic  $\mathbf{q} \neq 0$ -modal confinement, and (ii) predict a resulting *order-of-magnitude* high-temperature suppression of the perpendicular thermal transport. This reduction arises directly in the ratio  $\kappa_{\text{SL}}/\tau_{\text{SL}}$  and thus our work complements earlier investigations<sup>8,14</sup> of the effective superlattice phonon relaxation time  $\tau_{\text{SL}}$ . We emphasize that the (smaller) acoustic mismatch will drive a similar (but smaller) modal confinement and thermal conductivity reduction also in the GaAs/AlAs superlattices.<sup>6,7</sup>

Figure 1 characterizes our simple-cubic model of the double-silicon/double-germanium superlattice phonon dynamics. The upper panel shows one-dimensional model schematic assuming effective silicon/germanium lattice constants  $a_{\text{Si/Ge}}$  and atoms  $M_{\text{Si/Ge}}$  connected by intrasilicon/intragermanium force constants  $F_{p; \text{Si/Ge}}$  and interlayer coupling constants  $K_p \equiv \sqrt{F_{p; \text{Si}} F_{p; \text{Ge}}}$ .<sup>18</sup> This one-dimensional model, however, can only describe the dynamics of superlattice phonons both polarized ( $\xi_p \parallel \hat{z}$ ) and propagating exactly in the growth or  $\hat{z}$  direction.

The lower panel of Fig. 1 illustrates our simple-cubic model of the general superlattice phonon dynamics. We assume for simplicity a shared in-plane and perpendicular lattice constant,  $a \equiv a_{\text{Si}}$  (identical in all layers), and add in-plane force constants<sup>19</sup>  $F_{t; \text{Si/Ge}}$  necessary to describe the phonon propagation at a finite in-plane momentum  $\mathbf{q} \neq 0$ . We also introduce characteristic frequencies  $\Omega_{p,t; \text{Si(Ge)}} \equiv \sqrt{4F_{p,t; \text{Si(Ge)}}/M_{\text{Si(Ge)}}$ .

The  $\xi_p \parallel \hat{z}$ -polarized phonon modes at in-plane momenta  $\mathbf{q}$  is then described by a bulk silicon (germanium) model dispersion:

$$\omega_{\mathbf{q}}^2 = \Omega_{p; \text{Si(Ge)}}^2 [1 - \cos(k_{\text{Si(Ge)}} a)]/2 + \Omega_{t; \text{Si(Ge)}}^2 (\alpha_{\mathbf{q}}/2), \quad (1)$$

$$\alpha_{\mathbf{q}} = [2 - \cos(q_x a) - \cos(q_y a)] < 4, \quad (2)$$

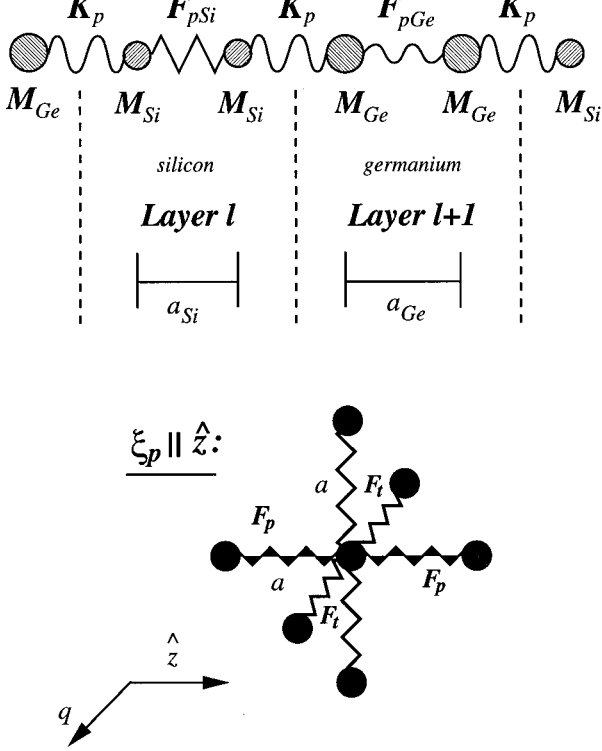


FIG. 1. Simple-cubic model for double-silicon/double-germanium superlattice phonon spectra. The upper panel shows one-dimensional model schematic with silicon/germanium atoms  $M_{\text{Si/Ge}}$  and lattice constants  $a_{\text{Si/Ge}}$ . The atoms are coupled by intrasilicon/intragermanium force constants  $F_{p;\text{Si/Ge}}$  and interlayer constant  $K_p \equiv \sqrt{F_{p;\text{Si}}F_{p;\text{Ge}}}$ . The lower panel illustrates the simple-cubic phonon model for the general  $\xi_p \parallel \hat{z}$ -polarized superlattice modes, that is, having a *nonzero* in-plane momentum,  $\mathbf{q} \neq 0$ . We assume a shared in-plane and perpendicular lattice constant,  $a \equiv a_{\text{Si}}$  (identical in all layers,) and add in-plane silicon/germanium force constants,  $F_{t;\text{Si/Ge}}$ .

relating frequency  $\omega_{\mathbf{q}}$  and perpendicular momentum  $k_{\text{Si(Ge)}}$ . We describe the bulk silicon (germanium) modes with polarization  $\xi_{\hat{x},\hat{y}} \parallel \hat{x},\hat{y}$  using the dispersion

$$\omega_{\mathbf{q},\hat{x},\hat{y}}^2 = \Omega_{t;\text{Si(Ge)}}^2 [1 - \cos(k_{\text{Si(Ge)}}a)]/2 + (\Omega_{p;\text{Si(Ge)}}^2 + \Omega_{t;\text{Si(Ge)}}^2)(\alpha_{\mathbf{q}}/4). \quad (3)$$

Silicon is significantly harder than germanium. Our simple model yields  $\Omega_{p;\text{Si(Ge)}} = 40.9$  (22.9) meV and  $\Omega_{t;\text{Si(Ge)}} = 28.3$  (16.5) meV and is not an accurate description of the longitudinal or transverse phonon modes.<sup>20</sup> However, the ratios  $\Omega_{p;t;\text{Si}}^2 \sim 3\Omega_{p;t;\text{Ge}}^2$  are consistent with the actual bulk phonon spectra and our model thus reflects the essential effects of the acoustic mismatch. Below we concentrate our discussion on the  $\xi_p$ -polarized modes.

Assuming perfect interfaces the in-plane momenta  $\mathbf{q}$  is conserved and thus characterizes also the superlattice modes together with the squared frequency value  $\omega_{\mathbf{q}}^2$ . The perpendicular dynamics of such a mode is described by the individual-layer model dispersion

$$\omega_{\mathbf{q};\text{Si/Ge}}^2 = \Omega_{p;\text{Si/Ge}}^2 [1 - \cos(k_{\text{Si/Ge}}a)]/2, \quad (4)$$

where  $\omega_{\mathbf{q};\text{Si/Ge}}^2 \equiv \omega_{\mathbf{q}}^2 - \Omega_{t;\text{Si/Ge}}^2(\alpha_{\mathbf{q}}/2)$  defines the effective squared frequency available for the perpendicular motion within the silicon/germanium.

A superlattice mode  $(\mathbf{q}, \omega_{\mathbf{q}}^2)$  will propagate (i.e., be characterized by a real wave vector  $k_{\text{Si/Ge}}$ ) through a silicon/germanium layer if and only if  $0 \leq \omega_{\mathbf{q};\text{Si/Ge}}^2 \leq \Omega_{p;\text{Si/Ge}}^2$ . In contrast, superlattice modes with  $\omega_{\mathbf{q};\text{Si(Ge)}}^2 < 0$  ( $> \Omega_{p;\text{Ge}}^2$ ) are germanium (silicon) confined by total internal reflection. For example, a high-energy mode with  $\omega_{\mathbf{q};\text{Si}}^2 \sim \Omega_{p;\text{Si}}^2$  yields a submonolayer decay length  $1/\gamma_{\text{Ge}}$  as may be estimated from

$$\cosh(\gamma_{\text{Ge}}a) \equiv (2\omega_{\mathbf{q};\text{Si}}^2/\Omega_{p;\text{Ge}}^2) - 1. \quad (5)$$

We describe the general phonon displacement field at  $\hat{z}$  coordinate  $j$  in layer  $l$  and in-plane momentum  $\mathbf{q}$  by

$$\eta_{\mathbf{q};l}(j) = A_l \exp(ik_l a j) + B_l \exp(-ik_l a j), \quad (6)$$

using either real or complex wave vectors  $k_l = \text{Si/Ge}$  for modes which in the silicon/germanium are propagating or evanescent, respectively. For the  $\xi_p \parallel \hat{z}$ -polarized modes the individual-layer displacement fields, Eq. (6), couple at the heterostructure interfaces through force constant  $K_p \equiv \sqrt{F_{p;\text{Si}}F_{p;\text{Ge}}}$ . The equation of motion for the two atoms bordering the  $l/l+1$  interface establishes the relation,  $(A_l, B_l) \leftrightarrow (A_{l+1}, B_{l+1})$ .<sup>12</sup>

Our four-atom superlattice has period  $d=4a$  and is described by the perpendicular superlattice phonon momentum  $k \in [-\pi/d, \pi/d]$ . We solve the equations linking  $(A_l, B_l) \leftrightarrow (A_{l+2}, B_{l+2})$  subject to the Bloch ansatz at  $k$ :

$$\eta_{\mathbf{q};l+2}(j+4) = \eta_{\mathbf{q};l}(j) e^{ikd}, \quad (7)$$

to obtain the frequency-squared values,  $\omega_{\mathbf{q};k,\lambda}^2$ ,  $\lambda = 1-4$ , and thus determine the (zone-folded) superlattice modal spectra (for  $\xi_p \parallel \hat{z}$ - as well as for  $\xi_{\hat{x},\hat{y}} \parallel \hat{x},\hat{y}$ -polarized modes.)

We assume a frequency-independent phonon relaxation time  $\tau_{\text{SL}}$  and denote by  $N(T)$  the Bose-Einstein distribution function at temperature  $T$ . Generalizing the Boltzmann equation result for bulk phonon transport<sup>21</sup> we evaluate the ratio of the perpendicular superlattice thermal conductivity  $\kappa_{\text{SL}}$  to phonon relaxation time  $\tau_{\text{SL}}$  using

$$\frac{\kappa_{\text{SL}}}{\tau_{\text{SL}}}(T) = \hbar \sum_m \left[ \int \frac{d^2 q}{(2\pi)^2} \int_{-\pi/d}^{\pi/d} \frac{dk}{2\pi} \times \sum_{\lambda} \omega_{\mathbf{q};k,\lambda} \left( \frac{\partial \omega_{\mathbf{q};k,\lambda}}{\partial k} \right)^2 \left( \frac{dN}{dT} \right) \right]. \quad (8)$$

Here the index  $m$  denotes a sum over polarization  $(\xi_p, \xi_{\hat{x},\hat{y}})$  and  $\lambda$  identifies the set of superlattice modes at  $m$ ,  $\mathbf{q}$ , and (zone-folded) perpendicular momentum  $k$ . The corresponding estimates,  $\kappa_{\text{Si/Ge}}/\tau_{\text{Si/Ge}}$ , for bulk silicon/germanium result by replacing in Eq. (8)  $d$  by  $a_{\text{Si/Ge}}$  and of course restricting  $\lambda$  to the single acoustic band described by our effective simple-cubic lattice model. Note that we divide out the very different phonon relaxation times,  $\tau_{\text{Si/Ge/SL}}$ , to obtain a fair comparison of the thermal conductivities and illustrate the superlattice effects.

Figure 2 compares the temperature variation of superlattice ratio  $\kappa_{\text{SL}}/\tau_{\text{SL}}$ , solid curve, with the corresponding estimates for bulk silicon, dashed curve, and for bulk germa-

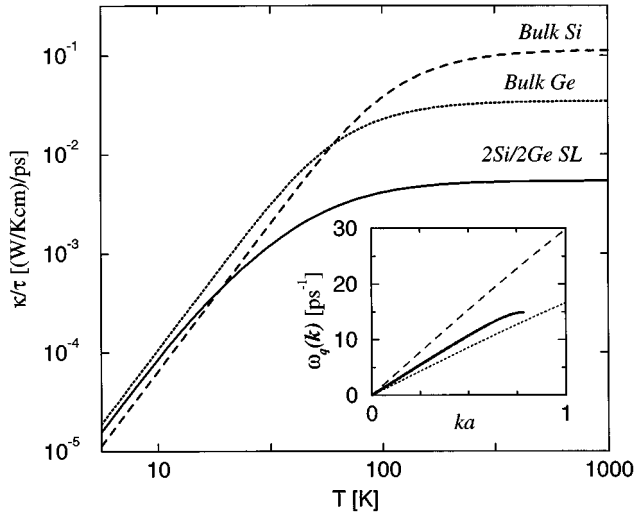


FIG. 2. Dramatic suppression of perpendicular superlattice thermal transport. The solid curve shows order-of-magnitude high-temperature reduction for calculated superlattice ratio of thermal conductivity ( $\kappa_{\text{SL}}$ ) to phonon relaxation time ( $\tau_{\text{SL}}$ ) when compared to average of bulk silicon/germanium ratios, dashed/dotted curve. The conductivity suppression results from the nonzero in-plane momenta  $\mathbf{q} \neq 0$  ensuring an effective confinement of the superlattice modes (Fig. 3). The inset verifies that no such confinement effect arises in the long-wavelength limit (relevant for the low-temperature transport): lowest  $\mathbf{q}=0$  superlattice spectrum, solid curve, is an average of corresponding Si/Ge spectra, dashed/dotted curves.

nius, dotted curve. To interpret this temperature variation of  $\kappa/\tau$  both for the superlattice and in the bulk we approximate  $\kappa$  as a product of the average group velocity,  $\langle \partial\omega/\partial k \rangle$ , average mean free path,  $\tau \langle \partial\omega/\partial k \rangle$ , and of the heat capacity,  $C$ :

$$\kappa \sim \tau \langle \partial\omega/\partial k \rangle^2 C/3. \quad (9)$$

In the low-temperature limit we may approximate the bulk silicon/germanium heat capacity,  $C_{\text{Si(Ge)}} \propto (T/\bar{v}_{\text{Si(Ge)}})^3$  where  $\bar{v}_{\text{Si(Ge)}}$  denotes the average long-wavelength sound velocity. Thus we have ratios  $\kappa_{\text{Si/Ge}}/\tau_{\text{Si/Ge}} \propto T^3/\bar{v}_{\text{Si/Ge}}$  yielding a cubic temperature dependence for the bulk materials. The low-temperature ratio  $\kappa_{\text{SL}}/\tau_{\text{SL}}$  is an average of  $\kappa_{\text{Si/Ge}}/\tau_{\text{Si/Ge}}$  because the long-wavelength superlattice velocity is an average of the Si/Ge velocities as documented in the inset of Fig. 2.

In contrast, the high-temperature ratio  $\kappa_{\text{SL}}/\tau_{\text{SL}}$  shows a dramatic suppression compared with the average bulk silicon/germanium values. This reduction reflects a suppression of the perpendicular average group velocity:

$$\kappa/\tau \propto \langle \partial\omega/\partial k \rangle^2; \quad T \gtrsim \Omega_{p,t;\text{Si/Ge}}, \quad (10)$$

as the high-temperature bulk silicon/germanium and superlattice heat capacities saturate at the Boltzmann constant times the density of phonon modes. To understand the dramatic reduction of the high-temperature ratio  $\kappa_{\text{SL}}/\tau_{\text{SL}}$  we investigate below the zone-folded superlattice phonon spectra

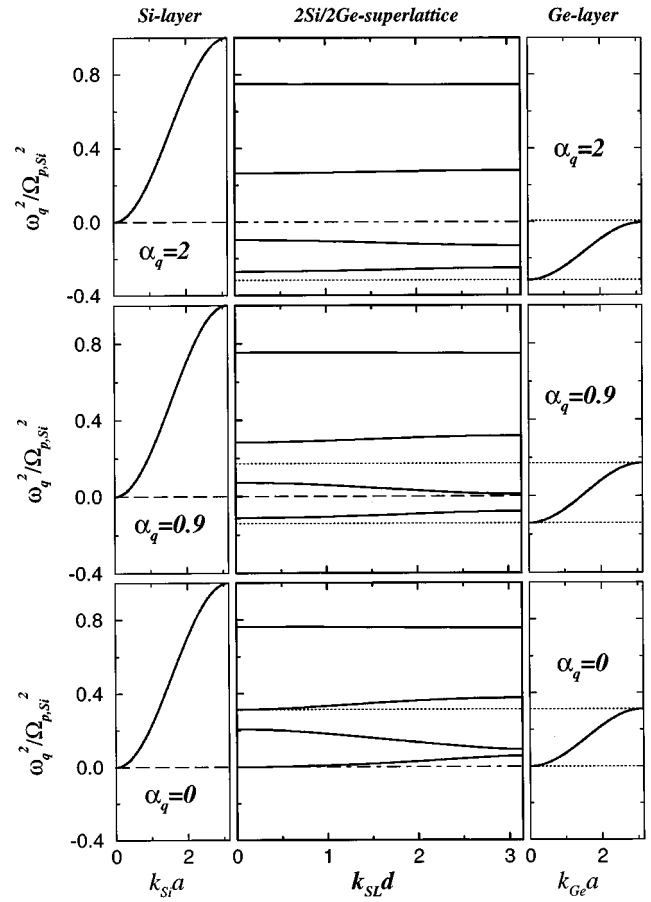


FIG. 3. Increasing silicon/germanium superlattice phonon confinement for upper/lower two zone-folded modes illustrated at  $\alpha_q \equiv [2 - \cos(q_x a) - \cos(q_y a)] = 0$  (bottom row), at  $\alpha_q = 0.9$  (middle row), and at  $\alpha_q = 2$  (top row). The central column of the panels shows the squared frequency values,  $\omega_q^2$ , of zone-folded superlattice modes ( $0 \leq k_{\text{SL}} d \leq \pi$ ). The left (right) column of panels compares with squared frequency values of modes able to propagate in bulk silicon (germanium),  $0 \leq k_{\text{Si(Ge)}} a \leq \pi$ . All panels show squared frequencies relative to  $\Omega_{t,\text{Si}}^2(\alpha_q/2)$  (dashed lines)—minimal value necessary for silicon propagation at  $\alpha_q$ . The dotted lines identify squared frequencies which at  $\alpha_q$  allow germanium propagation.

at general in-plane momenta  $\mathbf{q}$  and illustrate how the acoustic mismatch forces a significant reduction of the average phonon group velocity.

Figure 3 compares squared frequency values,  $\omega_q^2$ , for zone-folded superlattice modes, ( $0 \leq k_{\text{SL}} d \leq \pi$ ) central column, and for bulk-silicon/germanium propagating modes, ( $0 \leq k_{\text{Si(Ge)}} a \leq \pi$ ) left/right column, at increasing in-plane momentum  $\mathbf{q}$ . The bottom row of panels compares these phonon spectra at  $\alpha_q = 0$ , the middle row at  $\alpha_q = 0.9$ , and the top row at  $\alpha_q = 2$ . All panels show squared frequencies relative to  $\Omega_{t,\text{Si}}^2(\alpha_q/2)$  (dashed lines), minimal value necessary for propagation in the silicon. The pairs of dotted lines identify the range of squared frequency values which allows germanium propagation,  $0 \leq \omega_{\mathbf{q};\text{Ge}}^2 \leq \Omega_{p;\text{Ge}}^2$ .

The superlattice spectrum evaluated at  $\alpha_q = 0$ , central bottom panel, resembles the spectra obtained in previous one-dimensional theoretical studies.<sup>12,13</sup> The  $\alpha_q = 0$  dispersion curves show two modes which can propagate in all layers

and two modes located above the range of germanium-propagating modes. The top superlattice mode is almost entirely siliconlike. It is much too energetic to penetrate the germanium, and is consequently characterized by a vanishing group velocity.<sup>13</sup>

The intermediate value  $\alpha_{\mathbf{q}}=0.9$ , central *middle* panel, forces a finite offset between silicon- and germanium-propagating modes as identified by the set of dashed and dotted lines. The offset quantifies the traditional total internal effect: germanium phonons at a given  $\mathbf{q}\neq 0$  must have also a finite perpendicular momentum—that is, they must have more than the minimum energy set by  $\mathbf{q}\neq 0$ —to enter the harder silicon.

In turn this offset between the silicon- and germanium-propagating phonons causes a partial germanium confinement of the lowest superlattice mode and an increased silicon confinement of both upper two modes. Already at  $\alpha_{\mathbf{q}}=0.9$  we observe a significantly reduced contribution to the average superlattice phonon group velocity.

The central *top* panel illustrates how in-plane momenta with  $\alpha_{\mathbf{q}}\geq 2$  ensures a partial confinement of all superlattice phonon modes. The range of squared frequency values for modes propagating in the silicon (germanium) layers is at  $\alpha_{\mathbf{q}}=2$  situated entirely above (below) the dashed-dotted line. The top (bottom) two superlattice modes are thus at  $\alpha_{\mathbf{q}}\geq 2$

increasingly silicon- (germanium-) confined even by the thin adjacent germanium (silicon) layers.

The value  $\alpha_{\mathbf{q}}=2$  corresponds roughly to a minimal phonon energy of one half the germanium Debye temperature. At such temperatures and above the average modal confinement causes a dramatic suppression of the ratio  $\kappa_{\text{SL}}/\tau_{\text{SL}}$  as documented in Fig. 2.

We have theoretically investigated the thermal transport perpendicular to the interfaces in a double-silicon/double-germanium superlattice assuming a simple-cubic model for the lattice vibrations. We predict an order-of-magnitude high-temperature suppression in the ratio of the perpendicular thermal conductivity to the phonon relaxation time. This dramatic suppression occurs at temperatures above one half the germanium Debye temperature when the acoustic mismatch forces an effective modal confinement at the finite in-plane momenta  $\mathbf{q}$  characterizing this transport. Upon completion of this work we have learned of recent Si/Ge-superlattice measurements reporting perpendicular thermal conductivities *smaller* than that of an actual Si/Ge alloy.<sup>22</sup>

This work was supported by ARPA, the University of Tennessee, and the Division of Material Science, U.S. Department of Energy under Contract No. DE-AC05-96OR22464 with Lockheed Martin Energy Research Corporation.

\*Present address: Dept. of Elec. Eng., University of Notre Dame, Notre Dame, IN 46556.

<sup>1</sup>T. Yao, Appl. Phys. Lett. **51**, 1798 (1987).

<sup>2</sup>X. Y. Yu, G. Chen, A. Verma, and J. S. Smith, Appl. Phys. Lett. **67**, 3554 (1995).

<sup>3</sup>L. D. Hicks and M. S. Dresselhaus, Phys. Rev. B **47**, 12 727 (1993); G. D. Mahan and H. B. Lyon, Jr., J. Appl. Phys. **76**, 1899 (1994); J. O. Sofo and G. D. Mahan, Appl. Phys. Lett. **65**, 2690 (1994); D. A. Broido and T. L. Reinecke, Phys. Rev. B **51**, 13 797 (1995).

<sup>4</sup>P. Hylgaard and G. D. Mahan, in *Thermal Conductivity* (Technomic, Lancaster, PA 1996), Vol. 23, pp. 172–182.

<sup>5</sup>G. Chen, J. Heat Trans. **119**, 220 (1997).

<sup>6</sup>G. Chen, C. L. Tien, X. Wu, and J. S. Smith, J. Heat Trans. **116**, 325 (1994).

<sup>7</sup>W. S. Capinski and H. J. Maris, Physica B **219-220**, 699 (1996).

<sup>8</sup>G. Chen, in *Micro-Electro-Mechanical Systems* (ASME, New York, 1996), Vol. 59, pp. 13–24.

<sup>9</sup>K. Fuchs, Proc. Camb. Philos. Soc. **34**, 100 (1938).

<sup>10</sup>W. A. Little, Can. J. Phys. **37**, 334 (1959).

<sup>11</sup>V. Narayamurti, H. L. Stormer, M. A. Chin, A. C. Gossard, and W. Wiegmann, Phys. Rev. Lett. **43**, 2012 (1979).

<sup>12</sup>C. Colvard, T. A. Gant, M. V. Klein, R. Merlin, R. Fisher, H. Morkoc, and A. C. Gossard, Phys. Rev. B **31**, 2080 (1985).

<sup>13</sup>A. Fasolino, E. Molinari, and J. C. Maan, Phys. Rev. B **39**, 3923 (1989).

<sup>14</sup>S. Y. Ren and J. D. Dow, Phys. Rev. B **25**, 3750 (1982).

<sup>15</sup>R. A. Ghanbari, J. D. White, G. Fasol, C. J. Gibbings, and C. G. Tuppen, Phys. Rev. B **42**, 7033 (1990); A. Qteish and E. Molinari, *ibid.* **42**, 7090 (1990); S. de Gironcoli, *ibid.* **46**, 2412 (1992).

<sup>16</sup>M. I. Alonso, F. Cerdeira, D. Niles, M. Cardona, E. Kasper, and H. Kibbel, J. Appl. Phys. **66**, 5645 (1989); E. Molinari, S. Baroni, P. Giannozzi, and S. de Gironcoli, Phys. Rev. B **45**, 4280 (1992); S. de Gironcoli, E. Molinari, R. Schorer, and G. Abstreiter, *ibid.* **48**, 8959 (1993); R. Schorer, G. Abstreiter, S. de Gironcoli, E. Molinari, H. Kibbel, and H. Presting, *ibid.* **49**, 5406 (1994).

<sup>17</sup>We assume a radial interatomic potential and an equivalent simple-cubic geometry to which we adapt the description of phonons in nearest-neighbor face-centered-cubic materials; see N. W. Ashcroft and N. D. Mermin, *Solid State Physics* (Saunders College, Philadelphia, 1976), pp. 449–450.

<sup>18</sup>We choose effective lattice constants  $a_{\text{Si/Ge}}$  to fit actual mass densities, and force constants  $F_{p;\text{Si/Ge}}$  to yield simple-cubic sound velocity  $v_{p;\text{Si/Ge}}=(a_l\sqrt{F_{p;l}/M_l})_{l=\text{Si/Ge}}$  equal to the silicon/germanium values reported for [100] longitudinal phonons in H. Landolt and R. Börstein, *Numerical Data and Functional Relationships in Science and Technology*, New Series, 17e, (Springer-Verlag, Berlin, 1983), p. 63/397. In the long-wavelength limit this choice of effective parameters is consistent with the continuum-mechanics-based description of heterostructure phonon transmission probabilities, see for example S. Mizuno and S. Tamura, Phys. Rev. B **45**, 734 (1992).

<sup>19</sup>The force constants  $F_{r;\text{Si/Ge}}$  are fitted to the sound velocities of [100] *transverse* phonons in bulk silicon/germanium.

<sup>20</sup>H. Bilz and W. Kress, *Phonon Dispersion Relations in Insulators* (Springer-Verlag, Berlin, 1979), pp. 97–98.

<sup>21</sup>W. Jones and N. H. March, *Theoretical Solid State Physics* (Dover, New York, 1985), pp. 766–767.

<sup>22</sup>S. M. Lee, D. G. Cahill, and R. Venkatasubramanian, Appl. Phys. Lett. **70**, 2957 (1997).